Application of Shear-induced Diffusivity in Solid Particle Transportation: Experimental and Modeling

Ahmed Ramadan[1], Arild Saasen[2] and Pål Skalle[1]
[1]Department of Petroleum Engineering and Applied Geophysics, NTNU, N-7491 Trondheim, Norway
[2]Statoil, N-4035, Stavanger, Norway

ABSTRACT
This paper presents the results of erosion rate experiments and a solid particle transport model that employs shear-induced diffusivity. The tests were performed by eroding three types of sand beds with polymer solutions. The model predictions were found to be within an acceptable range. Applying shear-induced diffusivity improves the model.

INTRODUCTION

During the drilling of oil wells, the cuttings, generated by the drill bit at the bottom of the well are difficult to transport to the surface, especially when parts of the wellbore are horizontal. Solid particles and cuttings transportation is known to display a substantial non-uniform concentration profile, which influences hydraulic characteristics of the flow and has immediate concern for several fields of engineering. Suspension and transportation of solid particles in inclined pipes have been studied by employing hydrodynamic diffusion models. As a result, the study of non-Brownian type diffusion is becoming more useful and interesting for many of the solid transportation and hole cleaning studies. Hydrodynamic diffuison refers to the fluctuating motion of non-Brownian particles in a suspension, which occurs due to multi-particle interaction and/or turbulent velocity fluctuations. Turbulent flows are characterized by their ability to transport or mix momentum, kinetic energy and contaminants such as heat and particles. Taylor[2] introduced the concept of turbulent diffusion in a study of the spread of scalar properties such as smoke, heat or soluble matter. However, turbulent suspension flows with non-Brownian particles are still not completely understood, though they are very common in nature and various fields of science and engineering. Often the turbulent diffusivity in pipe and annular flows is assumed to have a parabolic profile; however, this hypothesis creates a serious problem. This is because with this assumption, the diffusivity coefficient becomes zero at the bed, creating a blocking layer there. As a result the turbulent diffusion coefficient is usually calculated at a small distance from the bed where the diffusion coefficient is high enough to suspend the bed particles. Based on experimental studies on sediment transport, Fredsøe[3] has recommended this distance to be twice the mean particle diameter of a bed. However, the application of this method can be very limited and may not work for cutting transport. Usually the drilling of oil wells is performed by using non-Newtonian fluids as a means of transport media for cuttings. Therefore, another method of estimating the diffusivity of solid particles very close the bed is necessary. Consequently, the present study employs shear-induced diffusivity to represent the mechanism of resuspension close to the bed.

MODEL DEVELPMENT

A convection-diffusion solid transport model presented here employs the sum of two diffusivities: shear-induced diffusivity and turbulent diffusivity. The model describes particle dispersion in pipe and annular flow as a phenomenon of the Fickian diffusion process. Accordingly, there is a random type movement of solid particles against the concentration or shear gradient. Resuspension and sedimentation are two of the phenomena that occur during solid particle transportation.

The following assumptions are made in the development of the model: 1) the inertial effect of the particles is neglected; 2) the fluid is assumed to have very low plasticity; 3) lateral diffusion is neglected; and 4) the particles are considered as molecules. The model compares upward resuspension flux with the downward sedimentation flux as shown in Fig. 1.

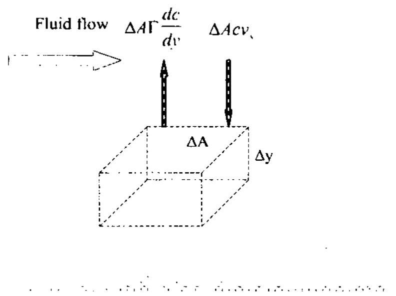

Figure 1. Resuspension and sedimentation fluxes.

If the problem of resuspension and sedimentation in the one-dimensional cross-section of a channel is considered, then the general convection-diffusion equation describing the particle resuspension in turbulent flow in the presence of gravity can be written as:

$$\frac{\Delta c \Delta y \Delta A}{\Delta t} = \Delta(\Gamma \frac{dc}{dy} + cv_s)\Delta A \quad (1)$$

where c is the solid particle concentration as a function of the distance from the solid bed y and time t; Γ is the total solid particle diffusion coefficient, v_s is the particle settling velocity. The total diffusivity coefficient is a function of the distance from the bed. The first term in the brackets is the diffusive term that represents the upward flux of solid particles by the action of turbulent eddies or other hydrodynamic interactions. And the second term represents the sedimentation flux of the particles due to gravitational force. In order to fulfill the steady state condition, the sum of terms in the brackets must be zero, yielding the steady state convection-diffusion equation written as:

$$\Gamma \frac{dc}{dy} = -v_s c \quad (2)$$

The total diffusivity coefficient is given by:

$$\Gamma = \Gamma_t + \Gamma_c + \Gamma_s \quad (3)$$

where Γ_t is the turbulent diffusivity coefficient. The shear-induced diffusivity coefficient against concentration gradient is represented by Γ_c, and Γ_s is an equivalent of shear-induced diffusivity coefficient against the shear gradient.

Theoretical and experimental studies on particle dispersion in turbulent flows indicate that the diffusivity of solid particles is roughly equal to or larger than the diffusivity of the fluid. The assumption that particle diffusivity is roughly equal to fluid diffusivity is also supported by theoretical results of homogeneous isotropic turbulence[4]. Moreover, the Reynolds analogy between heat or mass transport and momentum transport suggests that fluid diffusivity is same as eddy viscosity[5]. Therefore, the solid particle turbulent diffusivity coefficient is given by:

$$\Gamma_t = \kappa U_\tau (1 - y / D_y) y \quad (4)$$

where U_τ is the friction velocity given by $(\tau_w/\rho_f)^{0.5}$, D_y is characteristic length of the channel, κ is von Kármán constant. The bed shear stress τ_w is calculated using the Darcy-Weibach equation:

$$\tau_w = f_{bed} \frac{\rho_f U^2}{8} \quad (5)$$

where f_{bed} is friction factor of the bed.

In laminar flow particle transportation, two diffusive phenomena have been distinguished, these are self-diffusion and gradient diffusion[6]. Self-diffusion refers to a random fluctuation motion of a solid particle in a suspension undergoing shear where the particle concentration is uniform[7,8]. This type of diffusion does not induce a net particle migration. However, when a particle interacts with other surrounding particles, it experiences a series of displacements away from its original place. Even though the resultant of the displacements is zero, there is a finite mean square displacement which can be characterized by a shear-induced coefficient of self diffusion[9]. Therefore, as far as solids transportation is concerned, this type of diffusion has no importance.

On the contrary, the gradient diffusion can be very crucial for solid transportation when turbulent fluctuations are insignificant. Gradient diffusion can be from regions of high to low concentration and/or from regions of high to low shear. These types of hydrodynamic diffusions arise since a given particle in a sheared suspension experiences a greater amount of interaction from the high concentration side than from the other side or a greater amount of interaction from the highly sheared side than from the other side[9]. Even though gradient diffusion motion is irregular, it has a net migration effect from regions of high interaction to low interaction.

A theoretical analysis of flow in a horizontal circular pipe of an initially stratified with solid particles occupying the bottom portion of the pipe was made by Zhang[10] and Acrivos. They have expressed the particle flux from the bed to the fluid as:

$$N_d = -\Gamma_c \frac{dc}{dy} - D_s \frac{d\dot{\gamma}}{dy} \tag{6}$$

where D_s is shear-induced coefficient against shear stress gradient. Therefore, for channel flows the total shear-induced diffusivity coefficient can be expressed as:

$$\Gamma_{cs} = \frac{N_d}{(dc/dy)} = -\Gamma_c - D_s \frac{(d^2u/dy^2)}{(dc/dy)} \tag{7}$$

The term $D_s(d^2u/dy^2)/(dc/dy)$ is an equivalent shear-induced diffusion coefficient against the shear gradient, Γ_s which is introduced to compare the two types of shear-induced diffusion coefficients. The local flow velocity u for Xanthan Gum solution is estimated using the "law of the wall" presented by Kallio[14] and Reefs. Similarly, for PAC solution the velocity profile is estimated using a correlation presented by Bobok[15]. Zhang and Acrivos have presented an expression for the shear-induced diffusion coefficient against the concentration gradient as:

$$\Gamma_c = \frac{d_p^2}{4}\frac{du}{dy}\left(0.43c + 0.65c^2 \frac{1}{k_\mu}\frac{dk_\mu}{dc}\right) \tag{8}$$

where d_p is the particle diameter and k_μ is the relative suspension viscosity, which is the ratio of suspension viscosity to pure liquid viscosity and estimated using a relation developed by Krieger[11] as:

$$k_\mu = \left(1 - \frac{c}{c_m}\right)^{-1.82} \tag{9}$$

where c_m is a solid maximum packing fraction, which is set by previous studies to be 0.58[12]. Therefore, from Eqs. 8 and 9 we obtain a simplified relationship for the diffusion coefficient against the concentration gradient as:

$$\Gamma_c = \frac{d_p^2}{4}\frac{du}{dy}\left(0.43c + 2.04c^2\left(1 - \frac{c}{c_m}\right)^{-1}\right) \tag{10}$$

Similarly, an expression for an equivalent diffusion coefficient against the shear gradient can be written as:

$$\Gamma_s = 0.43c^2 \frac{d_p^2}{4}\frac{(d^2u/dy^2)}{(dc/dy)} \tag{11}$$

Determination of the settling velocity of the particles is necessary to solve Eq. 2. Settling has a negative impact on solid transportation and is mainly dependent on properties of the fluid and particles. Generally, a solid particle falling in a fluid under the action of gravity will accelerate until the drag force just balances gravitational force, after which it will continue to fall at constant velocity, which is given by:

$$v_s = \sqrt{\frac{4gd_p(\rho_s - \rho_f)}{3\rho_f C_D}} \tag{12}$$

where g is the gravitational acceleration, ρ_s is the particle density, ρ_f is the fluid density, and C_D is the particle drag coefficient that is determined by[13]:

$$C_D = \frac{24}{Re_p} + \frac{6}{1 + Re_p^{0.5}} + 0.4 \tag{13}$$

Equation 13 can be valid for Newtonian and non-Newtonian fluids if the definition of the particle Reynolds number is the same in both cases. Therefore, it is better to define the particle Reynolds number in a more general form as:

$$\mathrm{Re}_p = \frac{\rho_f v_s^2}{\tau} \qquad (14)$$

The shear stress, τ in the denominator will be determined by the rheological model of the fluid at representative shear rate v_s/d_p. After determining the settling velocity, Eq. 2, 3, 9, and 10 have been solved numerically using non-uniform grid elements in the vertical direction. Relatively very fine grid sizes are used near the bed. Actually an integrated form of Eq. 2 is employed in the numerical procedure, which is written as:

$$c_{i+1} = c_i e^{-\frac{v_s}{\Gamma_i}(y_{i+1}-y_i)} \qquad (15)$$

where c_{i+1} and c_i are concentrations at the top and bottom of a grid element; y_{i+1} and y_i are the vertical distances of the top and bottom of a grid element respectively.

FLOW LOOP EXPERIMENT

The experiments were conducted in a test section of a flow loop shown in Fig. 2. The test section is a 4 m long transparent pipe with internal diameter of 70 mm.

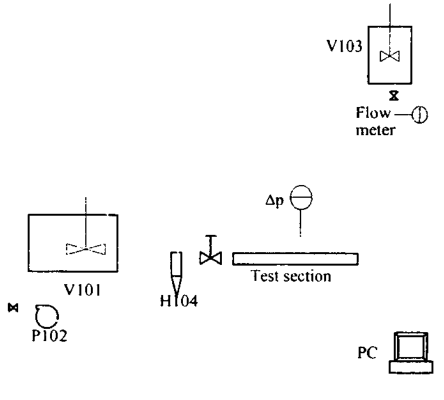

Figure 2. Flow diagram of the loop.

The flow loop is designed so that, at the test section, the flow is fully developed and free of any entrance effect. Aqueous solutions of Poly Anionic Celluloses (PAC) and Xanthan Gum polymers were prepared in a circulation tank V101. The solutions were circulated during the test runs by a centrifugal pump P102. The rheological properties of these solutions are presented in Table 1. The tests were performed by placing a sand sample in the test section uniformly and measuring the time of removal of the sand to when it is completely eroded; while the flow rate and pressure drop across the channel (test section) were recorded simultaneously. These two flow parameters were used to estimate the mean flow velocity and transport rates of the sample.

Table 1 Rheological parameters based on generalised Newtonian model.

Fluid	τ_y[Pa]	K [Pas^n]	n
PAC	-	0.050	0.7
Xanthan Gum	0.7	0.056	0.68

A hydrocyclone H104 was placed downstream of the test section to collect the removed sand. Steady gravitational flow through the test section was maintained by an overhead tank V103. Three types of sand beds with different particles size ranges were used during the test. The erosion test result for PAC with 1-liter sand bed is presented in Table 2.

Table 2. Erosion test result of PAC.

Particle size range [mm]	Mean velocity [m/s]	Time of removal [min]	Transport rate [kg/min]
0.5-1.2	0.86	7.8	0.17
0.5-1.2	0.94	6.0	0.22
0.5-1.2	1.03	2.6	0.49
0.5-1.2	1.11	1.5	0.87
2.0-3.5	0.70	25.8	0.05
2.0-3.5	0.78	9.6	0.14
2.0-3.5	0.86	1.6	0.81
2.0-3.5	1.01	0.7	1.78
2.0-3.5	1.12	0.6	2.20
4.5-5.5	0.61	24.0	0.05
4.5-5.5	0.69	12.5	0.10
4.5-5.5	0.78	2.1	0.63
4.5-5.5	0.86	1.0	1.30

For the Xanthan Gum solution test runs the erosion rates were measured indirectly by measuring the rate of change in the pressure drop. The result of the Xanthan Gum test is presented in Table 3.

Table 3. Results of Xanthan Gum tests.

Particle size range [mm]	Sand volume [lts]	Flow velocity [m/s]	d(Δp)/dt [Pa/s]	Transport rate [kg/min]
0.5-1.2	4.00	1.17	-6.45	0.93
2.0-3.5	4.00	1.00	-8.40	0.93
2.0-3.5	6.00	1.01	-6.00	0.80
4.5-5.5	1.00	1.32	-10.00	1.18
4.5-5.5	4.00	1.09	-6.50	1.11

MODEL PREDICTIONS

The convection-diffuison model not only estimates the transport rate but also predicts the concentration and shear-induced diffusivity profiles. Model simulations for the erosion of the beds were performed for the PAC solution with a mean fluid velocity of 1 m/s and 1-liter of sand bed; and presented in Fig. 3, 4 and 5. Model predicted concentration profiles of suspensions over the sand beds are presented in Fig. 3.

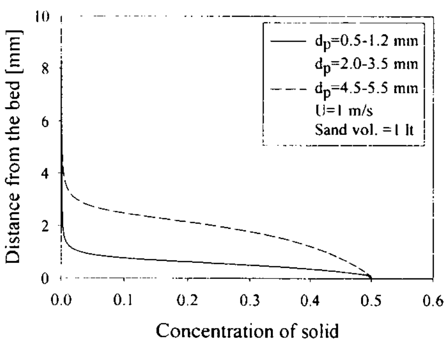

Figure 3. Concentration profiles for different sand beds.

According to the result in Fig. 3, the prediction indicates the existence of a highly concentrated dispersion layer on the surface of the bed. The presence of such a dispersed layer was observed during the flow loop test run. As seen from the figure the thickness of this layer increases with bed particle size and it is in the range of the particle size. When the thickness of this layer is less than the size of bed particles, the concentration profile becomes fictitious; however, this is not a serious problem because the particles are considered as molecules from the beginning. Furthermore, the presence of a highly concentrated dispersed layer supports the application of shear-induced diffusivity near the bed where the turbulent diffusivity is very small to suspend the particles.

In order to see the contribution of shear-induced diffusivity on the suspension of the particles, the profiles of the shear-induced diffusivity (diffusivity against concentration gradient) and turbulent diffusivity coefficients are presented in Fig. 4. As seen from this figure, the shear-induced diffusivity is very high near the bed but decays at a short distance from the bed. The two diffusivities become equal at small distance from the bed, which is in the range of the bed particle size in these cases. But this distance is not exactly the bed particle size. Therefore, the assumption of a highly diffusive layer near the bed with a thickness of twice the diameter of the bed particles is limited to the sediment transport and cannot be used for other transport conditions.

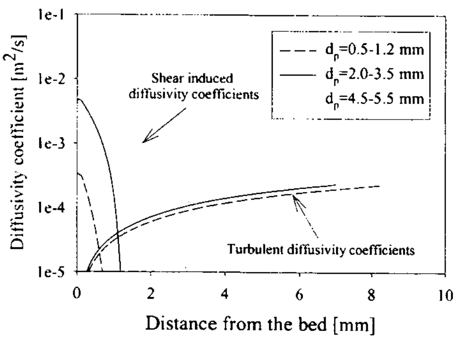

Figure 4. Shear-induced and turbulent diffusivity profile.

The simulation result also indicates the sensitiveness of shear-induced diffusivity to changes in bed particle size. But the variation of turbulent diffusivity due to the change in bed particle size is relatively small. For many near-bed diffusion rate calculations in the turbulent flow boundary layer, where the concentration gradient is high, the shear-induced diffusion coefficient against shear gradient is found to be negligible. In order to show the effect of this type of diffusion on the resuspension process, profiles of the two shear-induced diffusivity coefficients are presented in Fig.

5. The figure shows that the shear-induced diffusivity coefficient against shear gradient (Γ_s) is negligible when compared with the shear-induced diffusivity coefficient against concentration (Γ_c). However, the patterns of these two shear-induced diffusivities are similar.

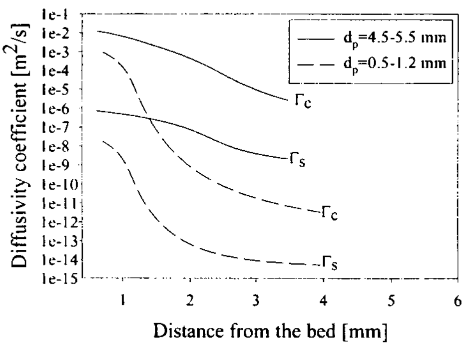

Figure 5. Shear-induced diffusivity profile for different sand bed sizes.

Finally it is important to compare transport rate predictions of the model with the measured data. Consequently, the measured data for Xanthan Gum solution are compared with the predictions of the model in Table 4.

Table 4. Transport rate comparison for Xanthan Gum solution test.

Particle size range [mm]	Model Prediction [kg/min]	Measured Data [kg/min]	Difference [%]
0.5-1.2	0.36	0.93	-61.76
2.0-3.5	0.34	0.93	-63.67
2.0-3.5	0.39	0.80	-50.77
4.5-5.5	2.81	1.18	138.51
4.5-5.5	1.70	1.11	52.70

As seen from Table 4, the predictions of the model are relatively higher for bed with coarser particles. This is probably due to the inertial effect of coarse particles and the plasticity of the fluid that reduce the accuracy of the model. The coarse bed changes the velocity profile; consequently, the shear-induced diffusivity will change significantly. Furthermore, the indirect erosion rate measurement may influence the result.

Measured transport rates from PAC test are also presented in Fig. 6 with the predictions of the model. Comparison of the model prediction with experimental results in Fig. 6 shows that the predictions of the model are relatively inaccurate for bed with coarser particles. As previously mentioned the inertial effect of coarse particles has significant impact on the accuracy of the model.

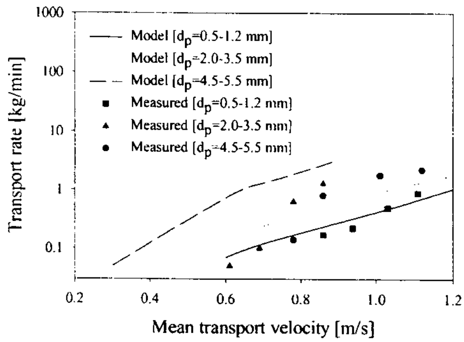

Figure 6. Transport rate versus mean velocity

Looking particularly at the measured data of PAC for particle size range of 0.5-1.2 mm, we see that the model predicts the transport rate reasonably for this particular sand bed. A detailed result from the model shows ever-increasing trend of the transport rate, as we increase the bed particle size. However, according to water test runs and theoretical analysis, there must be a critical particle size for a given flow velocity that gives the maximum transport rate. That means increasing the bed particle size beyond this particle size decreases the transport rate, so that it eventually reaches zero. This zero transport rate condition is a threshold condition for the resuspension process at that particular flow velocity and bed particle size.

CONCLUSION

The use of shear induced diffusivity coupled with turbulent diffusivity to estimate the concentration profile and transport rate improves the predictions and applicability of the convection diffusion model.

Shear-induced diffusivity is very strong near the bed and capable of resuspending the bed particle; however, this diffusivity declines very fast over a very short distance.

The contribution of shear-induced diffusivity against the shear gradient to the transport process is relatively small.

The convection diffusion based model can be applicable for resuspension and transportation of relatively fine bed particles.

PAC and Xanthan Gum solutions produce different rheologies, and the polymers are exposed to completely different degradation mechanisms. Moreover, the plasticity of a Xanthan Gum solution reduces the resuspension capability of the fluid.

ACKNOWLEDGEMENTS

The authors express their appreciation to the staff of the workshop and the laboratory at the Department of Petroleum Engineering at the Norwegian University of Science and Technology for their assistance in building the flow loop. The work was financed by Statoil, and we acknowledge their support.

REFERENCES

1. Tennekes, H. and Lumley, J.L. (1972) "A first course in turbulence", Mass MIT Press, Cambridge, pp. 8-14.
2. Taylor, G.I. (1921) "Diffusion by continuous movements", *Proceedings of the London Mathematical Society*, 2, 196-212.
3. Fredsøe, D. and Deigaard, R. (1992) "Mechanics of Coastal Sediment Transport", World Scientific Publishing Co., London, pp. 195-259.
4. Mohs, B., Mittendorff, I. and Oliemanns, R.V.A. (2000) "Results from a two-dimensional turbulent-model for dispersion and deposition of droplets in horizontal annular dispersed gas/liquid flow", *Int. J. Multiphase Flow,* 26, 6, 949-975.
5. Young, J. and Leeming, A. (1997) "A theory of particle deposition in turbulent pipe flow", *J. Fluid Mech.* 340, pp. 129-159.
6. Shams, M., Ahmadi, G. and Rahimzadeh, H. (2000) "A sublayer model for deposition of nano- and micro-particles in turbulent flows", *Chemical engineering science* 55, pp. 6097-6107.
7. Leighton, D. and Acrivos, A. (1987) " Measurement of shear-induced self-diffusion in concentrated suspensions of spheres", *J. Fluid Mechanics*, 177, pp. 109-131.
8. Davis, R.H. (1996) "Hydrodynamic diffusion of suspended particles: a symposium", *J. Fluid Mechanics*. 301, pp. 325-335.
9. Breedveld, V., VandenEnde, D., Tripathi, A. and Acrivos, A. (1998) " The measurement of the shear-induced particle and fluid tracer diffusivities in concentrated suspensions by a novel method", *J. Fluid Mechanics*. 375, pp. 297-318.
10. Zhang, k. and Acrivos, A.(1994) "Viscous resuspension in fully-developed laminar pipe flows", *Int. J. Multiphase Flow*, Vol. 20, No. 3, 579-591.
11. Krieger, I.M. (1972) "Rheology of monodisperse lattices", *Adv. Colloid Interface Science* 3, 111-136.
12. Leighton, D. and Acrivos, A.(1986) "Viscous resuspension", *Chem. Engineering Sci.*, 41, pp.1377-1384.
13. White, F. M. (1974) "Viscous Fluid Flow", McGraw-Hill, New York, pp. 200-210.
14. Kallio, G.A. and Reefs, M.W. (1989) "A numerical simulation of particle deposition in turbulent boundary layers", *Int. J. Multiphase Flow*, 15, 3, pp. 433-446.
15. Bobok, E. (1993) "Fluid mechanics for petroleum engineers", Elsevier Science Publisher B. V., Amsterdam, pp. 330-336.